ISSN 1028-334X, Doklady Earth Sciences, 2016, Vol. 466, Part 1, pp. 88–91. © Pleiades Publishing, Ltd., 2016.
Original Russian Text © Yu.V. Bataleva, Yu.N. Palyanov, Yu.M. Borzdov, O.A. Bayukov, N.V. Sobolev, 2016, published in Doklady Akademii Nauk, 2016, Vol. 466, No. 3, pp. 331–334.

GEOCHEMISTRY

The Formation of Graphite upon the Interaction of Subducted Carbonates and Sulfur with Metal-Bearing Rocks of the Lithospheric Mantle

Yu. V. Bataleva[a, b], Yu. N. Palyanov[a, b], Yu. M. Borzdov[a, b], O. A. Bayukov[c], and Academician N. V. Sobolev[a, b]

Received September 15, 2015

Abstract—Experimental studies of the Fe^0–(Mg, Ca)CO_3–S system were carried out during 18–20 h at 6.3 GPa, 900–1400°C. It is shown that the major processes resulting in the formation of free carbon include reduction of carbonates upon redox interaction with Fe^0 (or Fe_3C), extraction of carbon from iron carbide upon interaction with a sulfur melt/fluid, and reduction of the carbonate melt by Fe–S and Fe–S–C melts. Reconstruction of the processes of graphite formation indicates that carbonates and iron carbide may be potential sources of carbon under the conditions of subduction, and participation of the sulfur melt/fluid may result in the formation of mantle sulfides.

DOI: 10.1134/S1028334X16010190

Elements with a variable valence, such as Fe, S, and C, play an important role in magmatic and metasomatic processes in the Earth's mantle and have a key influence on the redox evolution of mantle rocks, melts, and fluids [1, 2]. As is shown in a number of modern studies of the global geochemical cycles of C and S [2–4], subduction is one of the main mechanisms of transportation of oxidized S and C forms into the reduced lithospheric mantle. In addition, modelling of various scenarios in the behavior of C- and S-bearing phases under the subduction environments are currently important [2, 3].

It is known that fO_2 in the different domains of the subcratonic lithospheric mantle may range from FMQ-1 to FMQ-5, however, with a basic tendency towards a decrease in the oxygen fugacity with depth [4, 5]. It is evident from experiments that the mantle becomes reduced at a depth of ~250 km, and the values of fO_2 decrease to the field of Fe^0 stability [6]. The probable interaction between the oxidized crustal material and reduced deep-seated rocks is supported by the data on inclusions in diamonds with the composition ranging from strongly reduced ones, such as metallic iron, moissanite, carbides, and sulfides, to oxidized ones including carbonates and sulfates [7–10]. The diamond-forming reactions of the interaction between carbonates and Fe^0-bearing mantle rocks have been studied [11], whereas the data on the potential role of sulfur in redox interactions under subduction environments are still limited.

Experimental studies of the Fe^0–(Mg, Ca)CO_3–S system were carried out on a multianvil split-sphere high-pressure apparatus (BARS) [12] during 18–20 h at a pressure of 6.3 GPa, a temperature range of 900–1400°C. Natural magnesite and dolomite (in a mole proportion of 8/1), Fe, and S (with a pureness of 99.99%) were used as the starting materials. The weights of carbonates, Fe^0, and S were 22, 43, and 8 mg, respectively. The traditional scheme of grinding and homogenization of the starting reagents was applied in ampoule preparation. Based on our previous experience in the study of sulfides and the mantle P–T conditions [13], we applied graphite as an optimal material for ampoules. The results of additional experiments in ampoules from talc ceramics are given in Table 1.

The phase and chemical compositions of the samples obtained were studied by the methods of energy-dispersive spectroscopy on a Tescan MIRA LMU scanning electron microscope and by microprobe analysis (a Camebax-micro microprobe). Phase relations in the samples were studied by the method of scanning electron microscopy. The composition of iron-bearing phases, the valent state of Fe in them, and the Fe distribution between the phases and nonequivalent sites was analyzed by the method of Mössbauer spectroscopy. The methodology of measure-

[a] *Sobolev Institute of Geology and Mineralogy, Siberian Branch, Russian Academy of Sciences, pr. Akad. Koptyuga 3, Novosibirsk, 630090 Russia*
[b] *Novosibirsk State University, Novosibirsk, 630090 Russia*
[c] *Kirenskii Institute of Physics, Siberian Branch, Russian Academy of Sciences, pr. Svobodny 79, Krasnoyarsk, 660036 Russia*
e-mail: bataleva@igm.nsc.ru

Table 1. Results of experiments in the Fe^0–(Mg, Ca)CO_3–S system at 6.3 GPa and 900–1400°C (the data of energy-dispersive spectroscopy)

Run no.	*T*, °C	*t*, h	Material of ampoule	Phases
1623-1	900	18	Gr	Po, Mws, Coh, Carb, Gr
1603-1	1000	18	Gr	Mws, Po, Coh, Gr
1620-1	1100	18	Gr	Mws, Po, Gr
1593-1	1100	20	Ta	Mws, Po, Ol, Gr
1619-1	1200	18	Gr	Mws, Po, Gr
1592-1	1200	20	Ta	Po, Ol, Gr
1599-1	1300	18	Gr	Mws, L_1, L_2, Gr
1618-1	1400	18	Gr	Mws, L_1, L_2, Gr

Hereinafter, Po, pyrrhotite; Mws, magnesiowüstite; Coh, cohenite; Carb, Fe, Ca, Mg carbonate; Gr, graphite; L_1, Fe–S–O melt; L_2, Fe–S–C melt; Ol, olivine; Ta, talc ceramics.

ments and analysis of the Mössbauer spectra is described in detail in [14].

The results of experiments and the chemical compositions of the phases are given in Tables 1–3. It is observed that the Fe^0–carbonate–S interaction at the lowest temperatures (900 and 1000°C) results in the formation of an association of pyrrhotite + Fe^{3+}-bearing magnesiowüstite + graphite + cohenite ± Fe,Ca,Mg-carbonate (Figs. 1a and 2). The main processes occurring at 900–1000°C include the interaction between the Fe and S melt/fluid resulting in crystallization of pyrrhotite and redox reactions between Mg,Ca-carbonates and Fe [11]. The interaction between carbonates and Fe^0 proceeds by the scheme

$$3(Mg, Ca)CO_3 + 5Fe^0 \rightarrow 3(Fe, Mg, Ca)O + Fe_3C + 2(Fe, Ca, Mg)CO_3, \quad (1)$$

whereas the newly formed carbide interacts with carbonate with the formation of an association of magnesiowüstite and graphite:

$$3(Mg, Ca)CO_3 + 2Fe_3C \rightarrow 9(Fe, Mg, Ca)O + 5C^0. \quad (2)$$

It is established that C^0 may appear in the form of graphite in the course of carbon extraction from carbide upon interaction with the S melt/fluid:

$$2Fe_3C + 3S_2 \rightarrow 6FeS + 2C^0. \quad (3)$$

As is shown by the method of Mössbauer spectroscopy, magnesiowüstite formed in association with graphite contains ~4 at % Fe^{3+}, which provides evi-

Table 2. Compositions of oxide and carbonate phases obtained in the course of Fe^0–carbonate–S interaction (data of microprobe analysis)

Run no.	*T*, °C	Phase	*N*	Composition, wt %					*n*(O)	Composition, arb. units				
				FeO	MgO	CaO	CO_2	Total		Fe	Mg	Ca	C	Total
1623-1	900	Mws	17	$77.2_{(27)}$	$20.7_{(27)}$	$1.8_{(8)}$	–	$99.8_{(3)}$	1	$0.66_{(4)}$	$0.32_{(3)}$	$0.02_{(1)}$	–	1.000
		Carb	10	$31.7_{(25)}$	$10.4_{(2)}$	$15.1_{(22)}$	$42.7_{(3)}$	$100_{(0)}$	3	$0.46_{(4)}$	$0.270_{(3)}$	$0.28_{(3)}$	$0.980_{(3)}$	$1.990_{(3)}$
1603-1	1000	Mws	14	$75.8_{(7)}$	$21.1_{(9)}$	$2.5_{(5)}$	–	$99.5_{(3)}$	1	$0.650_{(7)}$	$0.33_{(1)}$	$0.030_{(6)}$	–	1.000
1620-1	1100	Mws	13	$76.4_{(4)}$	$20.3_{(5)}$	$2.8_{(3)}$	–	$99.5_{(3)}$	1	$0.660_{(4)}$	$0.310_{(6)}$	$0.030_{(3)}$	–	1.000
1619-1	1200	Mws	12	$76.6_{(3)}$	$20.2_{(4)}$	$2.6_{(4)}$	–	$99.4_{(2)}$	1	$0.660_{(3)}$	$0.310_{(6)}$	$0.030_{(4)}$	–	1.000
1599-1	1300	Mws	12	$77.3_{(5)}$	$21.9_{(1)}$	$0.17_{(2)}$	–	$99.4_{(3)}$	1	$0.660_{(3)}$	$0.340_{(2)}$	$0.001_{(1)}$	–	1.000
1618-1	1400	Mws	10	$76.8_{(14)}$	$22.7_{(12)}$	$0.08_{(1)}$	–	$99.6_{(4)}$	1	$0.65_{(1)}$	$0.35_{(1)}$	$0.002_{(1)}$	–	1.000

Here and in Table 3, the average compositions are given; *N* is the number of analyses; 1σ standard deviation is given in parentheses ($77.2_{(27)}$ means 77.2 ± 2.7 wt %); *n*(O) is the number of oxygen atoms.

Table 3. Compositions of sulfide phases obtained in the course of Fe^0–carbonate–S interaction (the data of microprobe analysis and energy-dispersive spectroscopy)

Run no.	*T*, °C	Phase	*N*	Composition, wt %			
				Fe	S	O	Total
1623-1	900	Po	11	$63.4_{(2)}$	$36.2_{(2)}$	–	$99.68_{(3)}$
1603-1	1000	Po	10	$63.3_{(3)}$	$36.3_{(1)}$	–	$99.6_{(4)}$
1620-1	1100	Po	12	$63.3_{(3)}$	$36.3_{(1)}$	–	$99.6_{(4)}$
1619-1	1200	Po	14	$63.3_{(3)}$	$36.2_{(1)}$	–	$99.6_{(4)}$
1599-1	1300	L_1	15	$64.7_{(2)}$	$30.6_{(1)}$	$4.0_{(1)}$	$99.4_{(1)}$
		L_2	15	$66.0_{(13)}$	$35.1_{(8)}$	–	$99.7_{(2)}$
1618-1	1400	L_1	15	$65.4_{(3)}$	$29.2_{(4)}$	$5.4_{(3)}$	$100.0_{(2)}$
		L_2	15	$78.6_{(2)}$	$21.2_{(3)}$	–	$99.8_{(2)}$

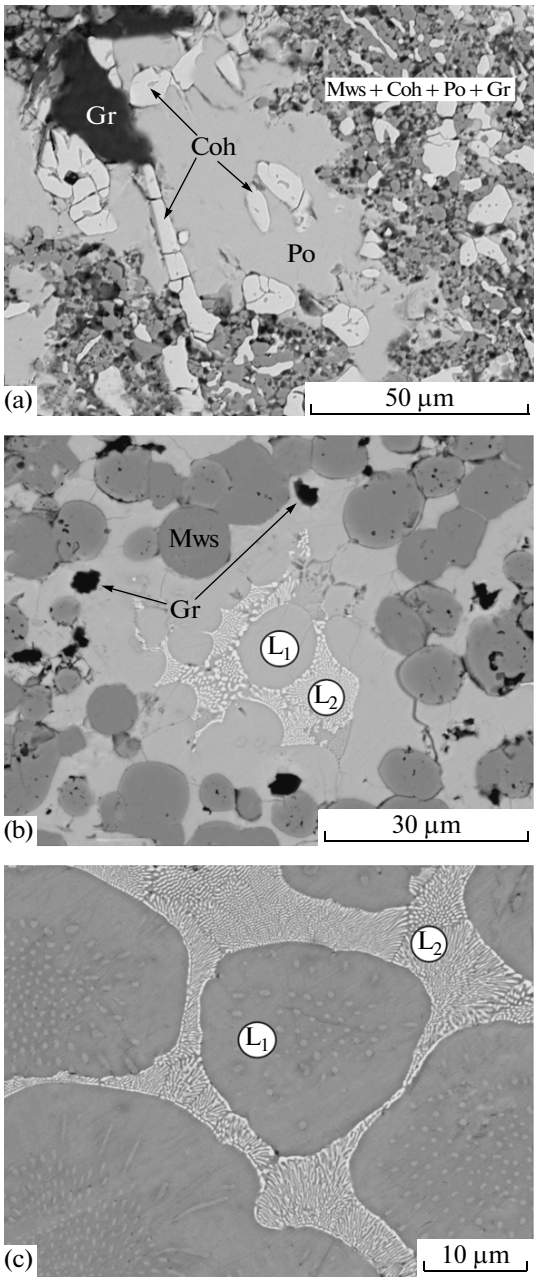

Fig. 1. SEM images: (a) polycrystalline aggregate of magnesiowüstite, cohenite, pyrrhotite, and graphite (1000°C); (b) magnesiowüstite and graphite crystals in a quenched aggregate (1300°C); (c) texture of quenched aggregate. Po, pyrrhotite; Mws, magnesiowüstite; Coh, cohenite; Gr, graphite; L_1, Fe–S–O melt; L_2, Fe–S–C melt.

dence for a probable redox interaction between magnesiowüstite and cohenite. This interaction results in Fe disproportionation:

$$(Fe, Mg, Ca)O + Fe_3C \rightarrow (Fe^{2+}, Fe^{3+}, Mg, Ca)O + C^0. \quad (4)$$

At 1100–1200°C, carbonates and Fe carbide are exhausted completely due to reactions (1)–(4) resulting in the formation of an association of pyrrhotite + Fe^{3+}-bearing magnesiowüstite + graphite. At $T \geq$ 1300°C, the processes of interaction in the Fe–carbonate–S system result in crystallization of Fe^{3+}-bearing magnesiowüstite and graphite and in the formation of two melts: Fe–S–O and Fe–S–C (Figs. 1b and 1c, Table 3). As is evident from the data of Mössbauer spectroscopy, a microdendritic aggregate of pyrrhotite and wüstite crystallizes from the Fe–S–O melt, and a microdendritic aggregate of Fe (with dissolved carbon) and pyrrhotite is formed from the Fe–S–C melt upon quenching (Fig. 1c). It is known that the formation of two immiscible melts (Fe–S and Fe–S–C) is observed in the Fe–S–C system at the same P–T parameters [15], whereas the reduced Fe–C melt and oxidized carbonate melt are formed in the carbonate–Fe system [11]. In the case of the more complex system Fe–carbonate–S, the carbonate melt participates in redox reactions with sulfide and metal–sulfide melts, which results in the formation of Fe–S–O and Fe–S–C melts, as well as in crystallization of Fe^{3+}-bearing magnesiowüstite and graphite.

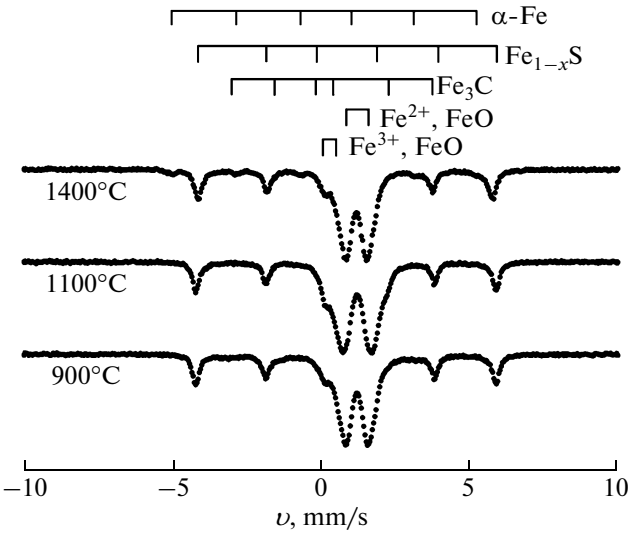

Fig. 2. Mössbauer spectra of the samples obtained during Fe^0–carbonate–S interaction.

Reconstruction of the processes of Fe–carbonate–S interaction shows that oxidation of Fe carbide in the redox interaction with carbonate (2) is the basic mechanism of graphite crystallization at $T \leq 1250$°C. Extraction of carbon from Fe carbide upon interaction with S melt/fluid (3) and the redox interaction of cohenite with magnesiowüstite (4) may be considered as additional scenarios of the formation of graphite in association with Fe^{3+}-bearing magnesiowüstite and pyrrhotite. It is established that the formation of graphite at higher temperatures proceeds through reduction of the carbonate melt by Fe–S and Fe–S–C melts.

Thus, the data obtained allow us to consider carbonates and Fe carbide as likely sources of carbon in the processes of graphite formation under the condi-

tions of subduction of oxidized crustal material into the reduced lithospheric mantle. The interaction between Fe^0 and carbonates in the presence of S-bearing melts/fluids resulting in the formation of elementary carbon in association with pyrrhotite and magnesiowüstite may be indicated by finds of polymineral inclusions in diamond represented by associations of sulfide + graphite, carbide + graphite, and wüstite + carbide + graphite [10]. It is established that the role of S in this interaction is not limited to the formation of mantle sulfides, but includes direct participation of S melts/fluids in the formation of free carbon, as well as the formation and redox evolution of Fe–S–O and Fe–S–C melts.

ACKNOWLEDGMENTS

This study was supported by the Russian Science Foundation (project no. 14-27-00054).

REFERENCES

1. R. W. Luth, *Mantle Petrology: Field Observations and High Pressure Experimentation: a Tribute to Francis R. (Joe) Boyd*, Ed. by Y. Fei, C. M. Bertka, and B. O. Mysen (Spec. Publ.–Geochem. Soc., Washington, 1999), Vol. 6, pp. 297–316.
2. R. Dasgupta, Rev. Mineral. Geochem. **75**, 183–229 (2013).
3. K. A. Evans, Earth Sci. Rev. **113**, 11–32 (2012).
4. S. B. Shirey, P. Cartigny, D. G. Frost, et al., Rev. Mineral. Geochem. **75**, 355–421 (2013).
5. A. B. Woodland and M. Koch, Earth Planet. Sci. Lett. **214**, 295–310 (2003).
6. A. Rohrbach, C. Ballhaus, U. Golla-Schindler, et al., Nature **449** (7161), 456–458 (2007).
7. N. V. Sobolev, E. S. Efimova, and L. N. Pospelova, *Geol. Geofiz.*, No. 12, 25–28 (1981).
8. E. S. Efimova, N. V. Sobolev, and L. N. Pospelova, Zap. Vses. Min. O-va **112** (3), 300–310 (1983).
9. I. S. Leung, Am. Mineral. **75**, 1110–1119 (1990).
10. G. Bulanova, J. Geochem. Explor. **53**, 1–23 (1995).
11. Yu. N. Palyanov, Yu. V. Bataleva, Yu. M. Borzdov, et al., Proc. Natl. Acad. Sci. U.S.A. **110** (51), 20408–20413 (2013).
12. Yu. N. Palyanov, Yu. M. Borzdov, A. F. Khokhryakov, et al., Cryst. Growth Des. **10**, 3169–3175 (2010).
13. Yu. N. Palyanov, Yu. M. Borzdov, Yu. V. Bataleva, et al., Earth Planet. Sci. Lett. **260**, 242–256 (2007).
14. Yu. V. Bataleva, Yu. N. Palyanov, Yu. M. Borzdov, et al., Russ. Geol. Geophys. **56** (1/2), 143–154 (2015).
15. L. Deng, Y. Fei, X. Liu, et al., Geochim. Cosmochim. Acta **114**, 220–233 (2013).

Translated by A. Bobrov